AMERICAN SOCIETY FOR MICROBIOLOGY | Journal of Virology®

VIRUS-CELL INTERACTIONS

Prazoles Targeting Tsg101 Inhibit Release of Epstein-Barr Virus following Reactivation from Latency

Sai Sudha Mannemuddhu,[a]* Huanzhou Xu,[b] Christopher K. E. Bleck,[c] Nico Tjandra,[d] Carol Carter,[e] Sumita Bhaduri-McIntosh[b,f]

[a]Department of Pediatrics, Division of Nephrology, University of Florida, Gainesville, Florida, USA
[b]Department of Pediatrics, Division of Infectious Diseases, University of Florida, Gainesville, Florida, USA
[c]Electron Microscopy Core Facility, National Heart, Lung, and Blood Institute, National Institutes of Health, Bethesda, Maryland, USA
[d]Laboratory of Molecular Biophysics, National Heart, Lung, and Blood Institute, National Institutes of Health, Bethesda, Maryland, USA
[e]Department of Microbiology and Immunology, Stony Brook University, Stony Brook, New York, USA
[f]Department of Molecular Genetics and Microbiology, University of Florida, Gainesville, Florida, USA

ABSTRACT Epstein-Barr virus (EBV) is a ubiquitous herpesvirus responsible for several diseases, including cancers of lymphoid and epithelial cells. EBV cancers typically exhibit viral latency; however, the production and release of EBV through its lytic phase are essential for cancer development. Antiviral agents that specifically target EBV production do not currently exist. Previously, we reported that the proton pump inhibitor tenatoprazole, which blocks the interaction of ubiquitin with the ESCRT-1 factor Tsg101, inhibits production of several enveloped viruses, including EBV. Here, we show that three structurally distinct prazoles impair mature particle formation postreactivation and identify the impact on stages of replication. The prazoles did not impair expression of lytic genes representative of the different kinetic classes but interfered with capsid maturation in the nucleus as well as virion transport from the nucleus. Replacement of endogenous Tsg101 with a mutant Tsg101 refractory to prazole-mediated inhibition rescued EBV release. These findings directly implicate Tsg101 in EBV nuclear egress and identify prazoles as potential therapeutic candidates for conditions that rely on EBV replication, such as chronic active EBV infection and posttransplant lymphoproliferative disorders.

IMPORTANCE Production of virions is necessary for the ubiquitous Epstein-Barr virus (EBV) to persist in humans and can set the stage for development of EBV cancers in at-risk individuals. In our attempts to identify inhibitors of the EBV lytic phase, we previously found that a prazole proton pump inhibitor, known to block the interaction of ubiquitin with the ESCRT-1 factor Tsg101, blocks production of EBV. We now find that three structurally distinct prazoles impair maturation of EBV capsids and virion transport from the nucleus and, by interfering with Tsg101, prevent EBV release from lytically active cells. Our findings not only implicate Tsg101 in EBV production but also identify widely used prazoles as candidates to prevent development of posttransplant EBV lymphomas.

KEYWORDS Epstein-Barr virus, viral inhibition, prazole, proton pump inhibitor, ESCRT, lytic cycle, Tsg101, ubiquitin

Epstein-Barr virus (EBV) is a double-stranded DNA virus of the gammaherpesvirus family (reviewed in reference 1). EBV establishes latent infection in B lymphocytes and remains dormant in the host. However, periodic switch into the lytic phase allows it to infect additional cells in the same host and to spread between human hosts. While this viral transition into the lytic phase is clinically silent in most hosts, the resulting virus production is an essential step in developing EBV-malignancies, such as posttransplant lymphoproliferative disease (PTLD) in the setting of immunosuppression. The incidence

Citation Mannemuddhu SS, Xu H, Bleck CKE, Tjandra N, Carter C, Bhaduri-McIntosh S. 2021. Prazoles targeting Tsg101 inhibit release of Epstein-Barr virus following reactivation from latency. J Virol 95:e02466-20. https://doi.org/10.1128/JVI.02466-20.

Editor Richard M. Longnecker, Northwestern University

Address correspondence to Carol Carter, carol.carter@stonybrook.edu, or Sumita Bhaduri-McIntosh, sbhadurimcintosh@ufl.edu.

* Present address: Sai Sudha Mannemuddhu, East Tennessee Children's Hospital, University of Tennessee, Knoxville, Tennessee, USA.

Received 29 December 2020
Accepted 31 March 2021
Accepted manuscript posted online 14 April 2021
Published 10 June 2021

of PTLD, which can have devastating consequences, ranges between 1 and 10% depending on the type of transplant and the degree of immunosuppression. To date, an EBV-specific antiviral capable of reducing EBV load during immunosuppression or a specific vaccine is unavailable.

Many enveloped viruses recruit the endosomal sorting complex required for transport (ESCRT) pathway for viral budding (2, 3). One of its components, tumor suppressor gene 101 (Tsg101), was shown to play an important role in egress of human immunodeficiency virus (HIV), also an enveloped virus (4–7). By disrupting Tsg101 interaction with ubiquitin (Ub), prazoles inhibit the production of HIV-1 and several other enveloped viruses, including EBV (8). Prazoles are FDA-approved prodrugs that are used widely to treat gastroesophageal reflux disease (GERD) (9). Ub is a 76-amino-acid polypeptide that is added to primary amino groups of acceptor proteins and plays both known and unknown roles in cellular cargo sorting, signaling, and enveloped virus budding. As Ub, the Ub ligase Itch, and the ESCRT adaptor protein ALIX have been implicated in regulating EBV BFRF1- and BFLF2-mediated modification of the nuclear envelope, thereby facilitating transport of immature capsids from the nucleus to the cytoplasm (10, 11), we hypothesized that the sensitivity of EBV production to prazoles might be linked to their interference with Tsg101 Ub binding. Alix and Tsg101 both function as ESCRT-III recruiters.

Ub modification of proteins requires the activity of a cascade of E1, E2, and E3 enzymes that sequentially activate the peptide (E1), conjugate it (E2) to mediate its transfer to the ligating enzyme (E3), and then covalently add it to the substrate. Tsg101 is an enzymatically inactive homolog of ubiquitin-conjugating (E2) enzymes (12, 13). Though still able to bind Ub via a pocket within its N-terminal Ub E2 variant (UEV) domain, the protein cannot transfer Ub to E3 ligases, as it lacks the active-site Cys residue necessary to form a transient thioester bond with the C terminus of Ub. Tsg101 facilitates recognition of cargo that is to be sorted in the endosomal pathways, e.g., for delivery to a degradative compartment, the plasma membrane or some other compartment, and this role is believed to be facilitated through its Ub binding (2–8, 14). Through another pocket, also in the UEV domain, Tsg101 recognizes short P(T/S)AP motifs in proteins that recruit it, such as the HIV precursor polyprotein Gag. Although the Tsg101-PTAP interaction is required for interaction with Gag (5–7), Tsg101-Ub and Tsg101-RNA binding are essential for recruitment of the ESCRT machinery to virus assembly sites on the plasma membrane and for HIV budding (15–17). Importantly, prazoles interact with the UEV domain to block Tsg101-Ub binding, thereby impairing HIV release (8, 15). Based on our recent discovery that a prazole inhibits EBV egress (8), we investigated the effects of diverse prazoles on the lytic phase of EBV and found that all of the drugs interfered with EBV capsid maturation and exit from the nucleus. Inhibition of virus production was reversed when the pool of endogenous Tsg101 was depleted and replaced with Tsg101 that had been made impervious to prazole attack by mutation of the UEV Cys residue targeted by the compounds. We conclude that Tsg101-Ub binding may be critical for recruitment of the membrane remodeling apparatus at the nuclear membrane as well as at the plasma membrane. Our findings also identify prazole compounds as potential therapies for EBV diseases.

RESULTS AND DISCUSSION

Related prazoles inhibit EBV release from lytically induced cells. We assessed the effect of three related but structurally distinct prazoles (tenatoprazole [T], ilaprazole [I], and rabeprazole [R]) on release of EBV from cells, using a well-established system for studying the EBV lytic phase. Prazole compounds are highly effective inhibitors of HIV-1 replication but exhibit different levels of efficacy (8, 15). As in the parental Burkitt lymphoma cell line HH514-16, EBV in CLIX-FZ cells is tightly latent but readily undergoes transition into the lytic phase when exposed to doxycycline; doxycycline activates the stably integrated EBV *BZLF1* gene, which encodes the viral lytic switch protein ZEBRA (18, 19). ZEBRA expression permits the effects of prazoles on the lytic phase to be evaluated without the confounding presence of a broadly acting lytic-inducing

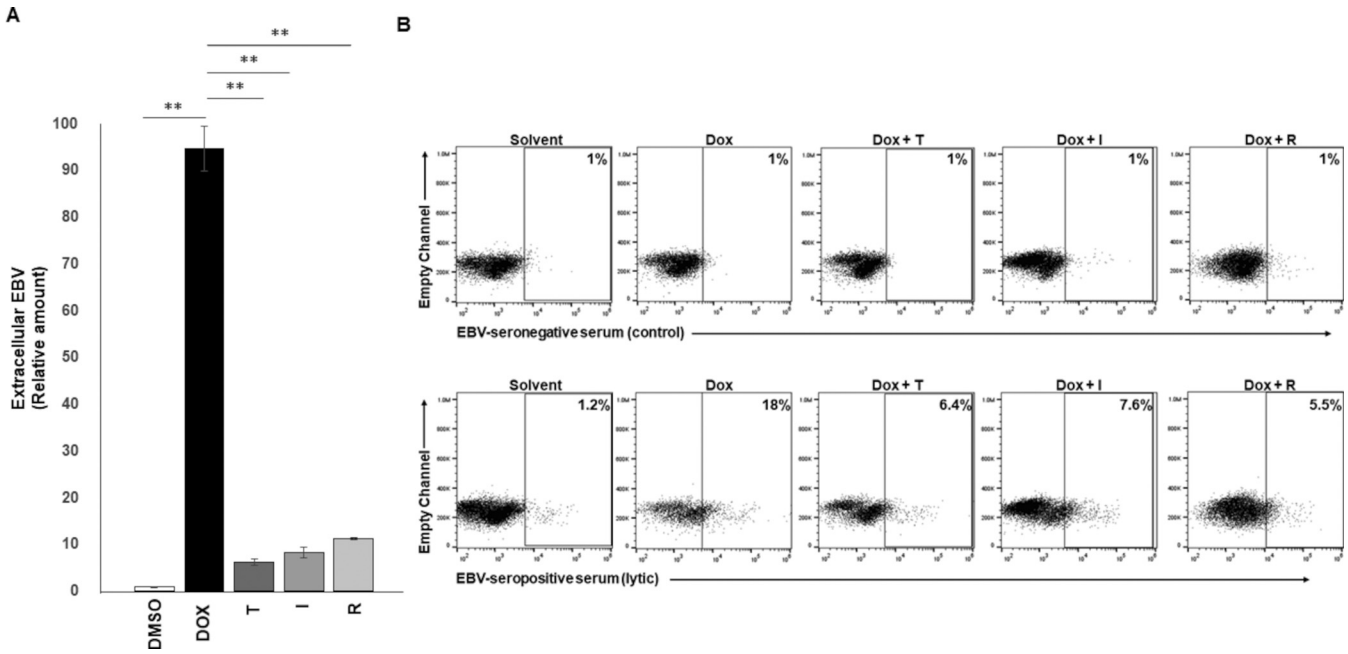

FIG 1 Prazoles inhibit EBV release from lytically induced cells. CLIX-FZ BL cells were exposed to doxycycline to activate the lytic phase of EBV (Dox) or Dox plus prazoles (T, tenatoprazole; I, ilaprazole; R, rabeprazole). (A) Culture supernatants were harvested 72 h later, treated with DNase, and assayed for EBV load using qPCR. **, $P < 0.001$. Error bars show standard errors of the means (SEM) for biological triplicates. (B) Cells were harvested at 48 h and surface stained using reference EBV-seronegative control serum (top) or reference EBV-seropositive serum to identify lytically active cells (bottom).

agent such as a histone deacetylase (HDAC) inhibitor. As shown in Fig. 1A, exposure to doxycycline resulted in a significant increase in detection of DNase-resistant virus in the culture supernatant. Treatment with T, I, and R knocked down the amount of virus detected by ~90%. In a complementary approach, we used a previously validated EBV-seropositive serum (compared to a control EBV-seronegative serum) to detect lytic virus on the surface of live cells using flow cytometry (20, 21). We found that, consistent with the results of Fig. 1A, treatment with prazoles resulted in 60 to 70% reduction in detection of cells with lytic virus on the surface (Fig. 1B). That said, prazoles appeared to be more effective in the extracellular DNA assay than in the flow cytometry assay. This difference results from the following inherent differences between the two assays: (i) the PCR-based assay measures encapsidated viral genomes, while the flow-based assay measures the number of cells producing virus particles, and (ii) any empty virions, i.e., virions lacking viral genomes resulting from prazole treatment, would not be captured by the PCR assay but would still be detected as virus particles in the flow assay. Collectively, these findings indicate that prazoles inhibit release of EBV from lytically active cells. Furthermore, the impact of the three compounds was comparable. In that regard, tenatoprazole exhibited a 50% effective concentration (EC_{50}) of $<20\ \mu$M for EBV compared to 50 μM for HIV-1 and 3.2 μM to function as a proton pump inhibitor (8). Ilaprazole and rabeprazole were as effective as tenatoprazole at 10 μM; ilaprazole exhibits an EC_{50} of 6 μM for proton pump inhibition (22).

Prazoles do not impair EBV lytic gene expression. A key step in virus production is lytic gene expression. Lytic gene expression is a temporally regulated process in which the lytic switch ZEBRA (and another immediate early lytic gene product, RTA) turn on expression of early lytic genes whose products are essential for replication of EBV genomes. Genome replication is followed by expression of late lytic genes, whose products largely contribute to structural components of the virus. In our system, ZEBRA expression was turned on from an exogenous *BZLF1* locus, making it difficult to differentiate between exogenous and endogenous *BZLF1* transcripts. We therefore determined the effect of prazoles on representatives of early and late gene expression. None of the prazoles T, I, and R blocked expression of *BMRF1*, a representative early

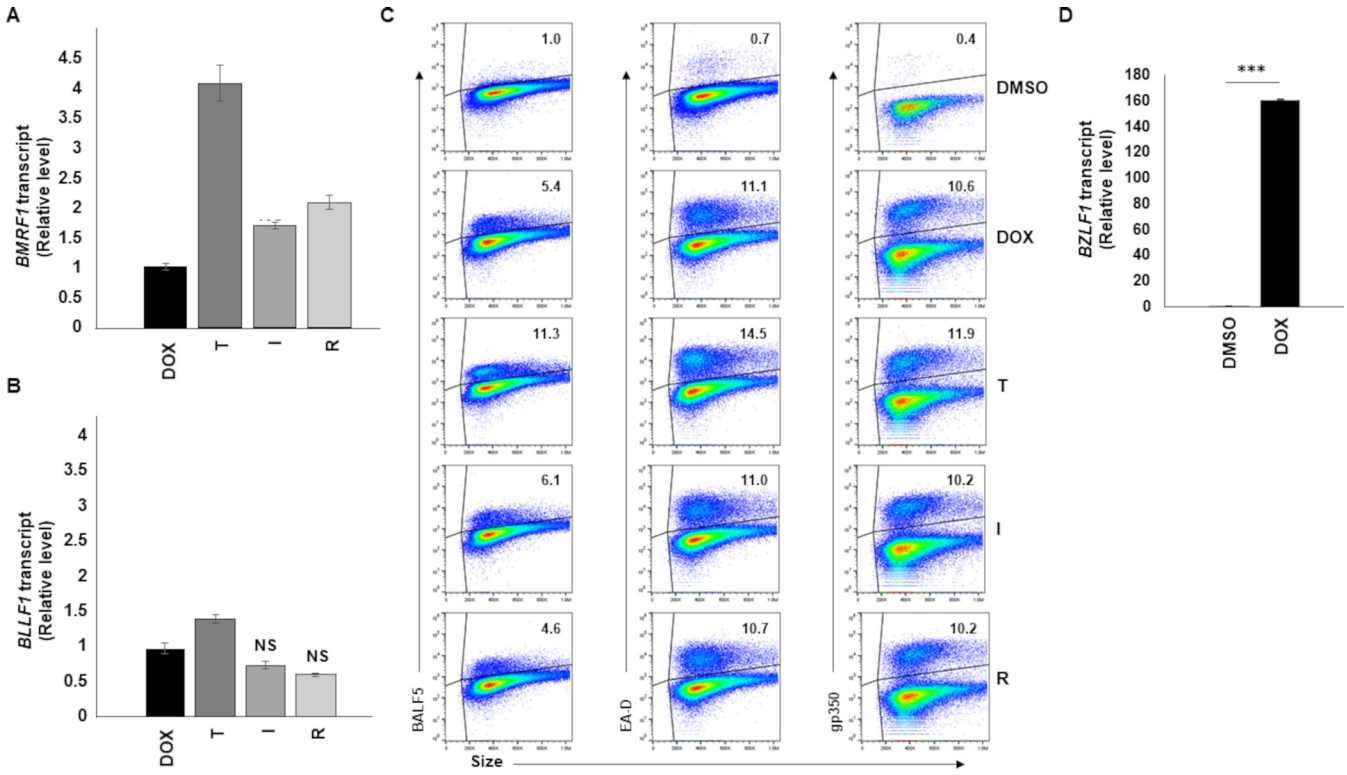

FIG 2 Prazoles do not block EBV early and late lytic gene expression. CLIX-FZ cells were treated with DMSO, doxycycline to induce the lytic phase of EBV (Dox), or Dox plus prazoles (T, tenatoprazole; I, ilaprazole; R, rabeprazole). Cells were harvested 72 h later (or 48 h later [D]) and assayed for *BMRF1* transcript (A) or *BLLF1* transcript (B) using RT-qPCR, for expression of BALF5, EA-D, and gp350 by flow cytometry (C), or for intracellular viral genomes using qPCR to amplify the *BALF5* gene (D). Error bars in panels A, B, and D show SEM for three technical replicates. *, $P < 0.05$; **, $P < 0.01$; ***, $P < 0.001$; NS, no significant reduction compared to Dox alone; gates in flow cytometry plots were determined by comparison to isotype control stained cells. Experiments were performed twice.

lytic gene whose product serves as the DNA polymerase processivity factor, or *BLLF1*, a representative late lytic gene that encodes the major EBV glycoprotein gp350 (Fig. 2A and B). Confirming these findings, prazoles did not inhibit steady-state levels of EA-D (*BMRF1* gene product), BALF5 (the viral DNA polymerase; a product of the early lytic gene *BALF5*), or gp350 proteins. Indeed, neither the percentage of cells expressing these viral proteins nor their levels in individual cells were impaired (Fig. 2C). Although T seemed to have a slightly positive effect on the levels of BALF5 and EA-D, the effect on gp350 steady state was negligible. As expected, treatment with doxycycline resulted in a significant (~160-fold) increase in *BZLF1* transcripts (Fig. 2D). These results indicate that expression of lytic genes, including postreplication lytic genes, is not negatively impacted by prazoles.

To ensure that prazoles did not adversely alter the metabolic state of cells, we tested the three drugs on CLIZ-FZ BL cells and A549 (human alveolar basal epithelial adenocarcinoma) cells and found no difference in metabolic activity after exposure to prazoles (Fig. 3A and B).

These results support the conclusion that the effect of the prazoles is highly selective: under conditions of minimal interference with cellular metabolism or EBV early or late lytic gene expression, prazoles interfere significantly with EBV's egress, a postreplication event.

Prazoles impair egress of EBV capsids from the nucleus. Ubiquitination of endocytic cargo signals Tsg101 in ESCRT-I to ultimately recruit ESCRT-III to sites of cargo accumulation on endocytic or plasma membranes which triggers membrane reformation and scission, important steps in cytokinesis, multivesicular body (MVB) formation, nuclear membrane remodeling, and virus budding (23, 24). EBV utilizes this membrane remodeling machinery for the formation of primary capsid envelopment, tegument acquisition and secondary envelopment while budding from the nuclear membrane, transport

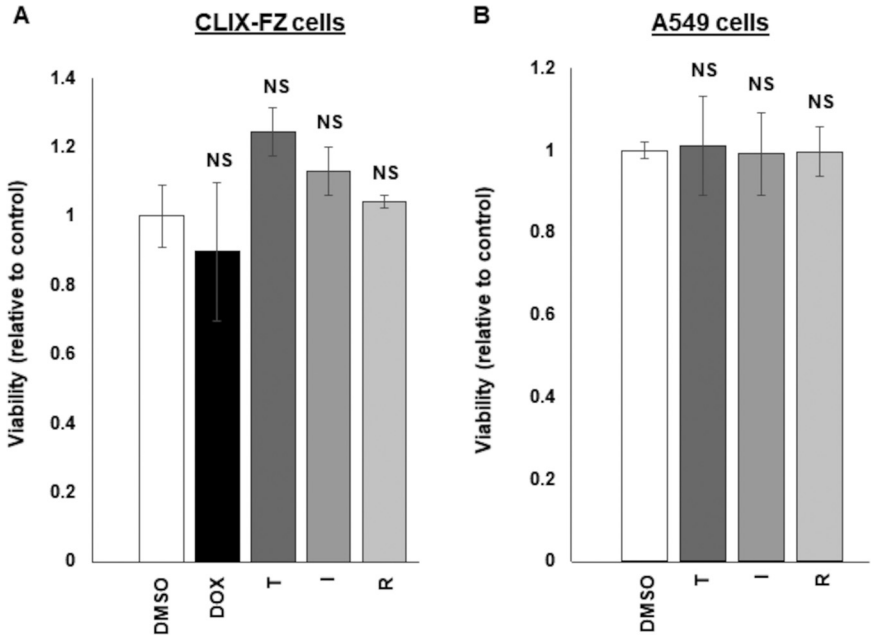

FIG 3 Prazoles demonstrate minimal toxicity. CLIX-FZ BL (A) and A549 (B) cells were exposed to DMSO, doxycycline (Dox [A]), or Dox plus prazoles (T, tenatoprazole; I, ilaprazole; R, rabeprazole) and harvested 24 h later for assessment of viability using the WST-1 assay. NS, not significant. Error bars show SEM for technical triplicates. The experiment was performed twice.

through the cytoplasmic membranes, and ultimately cell egress (25). Following activation of the lytic cycle, immature virus buds through the inner nuclear membrane, facilitated by ubiquitination (10). Once EBV matures in the cytoplasm, it leaves the cell via exocytosis. Interruption of these processes could therefore prevent virus egress and/or result in viruses with incomplete membranes, thus rendering them ineffective to infect new cells.

To visualize the effects of prazoles on EBV morphology and localization, we used electron microscopy. As expected, there were no virus particles in cells prior to lytic induction (Fig. 4A). As also expected, activating the lytic cycle with doxycycline resulted in detection of a large number of virus-like particles (VLPs) resembling immature capsids in the nucleus (Fig. 4B). The nuclear VLPs exhibited two main morphologies, a single shell with electron dense center and a double shell without center density (indicated by cartoons in Fig. 4B). Activating the lytic cycle in the presence of prazoles resulted in detection of VLPs exhibiting similar morphologies in the nucleus. However, in addition, particles possessing single shells but lacking central density were detected with greater frequency than in the absence of prazoles (compare Fig. 5A and Fig. 4B). Indeed, there were 55.5% defective/empty capsids observed in the presence of prazoles compared to 31% in the presence of doxycycline alone (Fig. 5D). Furthermore, consistent with observations made with HSV-1 and HSV-2 (26), following doxycycline treatment, nuclear EBV VLPs measured ~100 nm in diameter, in contrast to extracellular virions, which measured ~200 nm (Fig. 4B and C). In contrast, while nuclear VLPs measured close to 100 nm, virions detected outside cells exposed to prazole were smaller than their counterparts released from non-prazole-treated cells, measuring 100 to 150 nm (Fig. 5A to C). These findings suggest that prazoles interfere with capsid maturation in the nucleus and the cytoplasm as well as with exocytosis of mature particles.

The prazole-mediated interference reflects targeting of Tsg101 Cys73. Previous studies indicated that prazoles disrupt the interaction between Ub and Tsg101 within the UEV domain (15). Possibly by analogy to Alix (10, 11), Tsg101-Ub binding participates in BFRF1/BFLF2-mediated functions during EBV maturation. To test this, we asked whether the prazole-mediated defect in EBV egress was related directly to the ability of prazoles to block Tsg101 function. We previously demonstrated that prazole

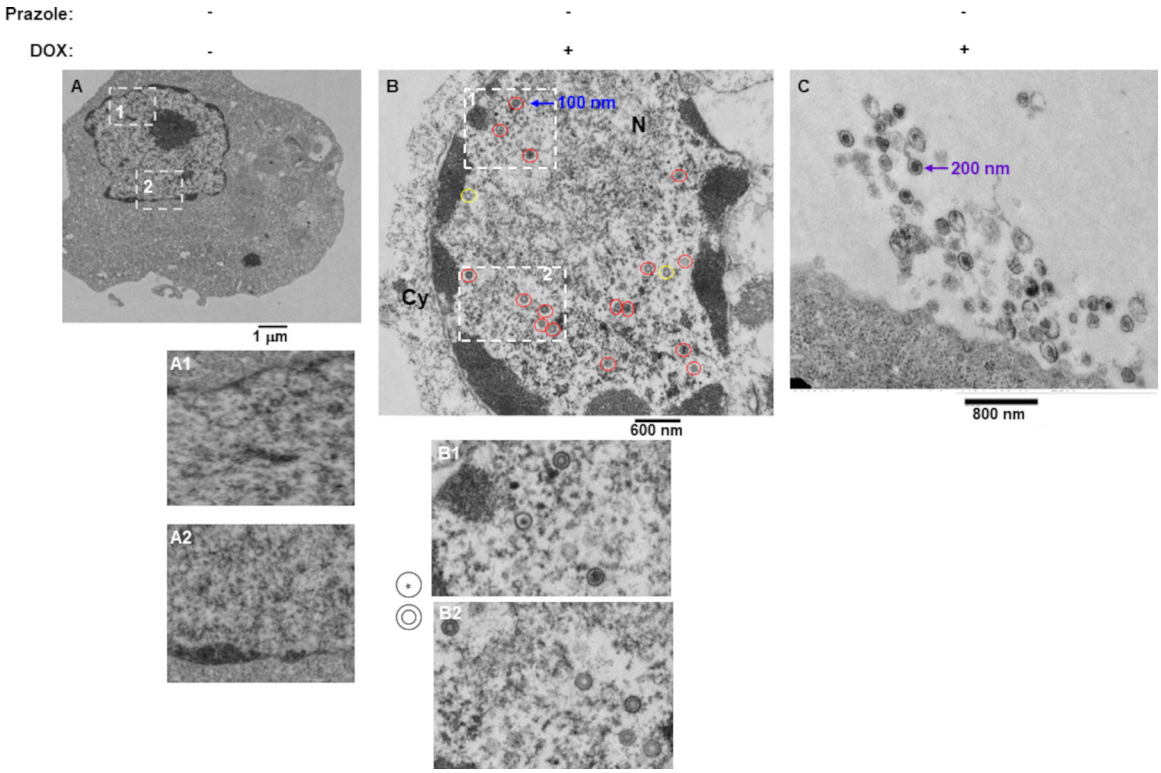

FIG 4 VLPs are detected in the nucleus and the extracellular space following lytic activation from latency. CLIX-FZ BL cells were exposed to DMSO (A) or doxycycline (Dox) (B and C). Cells were harvested 48 h later for evaluation by electron microscopy. Nuclei in panels A, A1, and A2 demonstrate a general lack of VLPs. (B) Dox-treated cells show numerous VLPs in the nucleus. Cartoons next to panels B1 and B2 indicate two predominant morphologies of nuclear VLPs (circled in red in panel B); those circled in yellow in panel B indicate defective-appearing VLPs with a single shell that lack a central electron-dense material. (C) Dox-treated cells show numerous extracellular virions. Sizes of nuclear and extracellular VLPs are indicated in panels B and C.

metabolites disrupt Tsg101 Ub binding by forming a disulfide linkage with cysteine 73 in the Tsg101 UEV domain (8, 15). Mutation of cysteine 73 to alanine (C73A) makes Tsg101 refractory to prazole targeting without any detectable deleterious effect on Tsg101 function. We therefore depleted the pool of endogenous Tsg101 protein using a previously validated small interfering RNA (siRNA)-targeting strategy (15) in cells expressing ectopic FLAG-tagged wild-type or C73A-mutated Tsg101 in EBV$^+$ p2089 cells. These are HEK-293T-derived cells that carry the EBV genome and, like latently infected B cells, do not express lytic genes at baseline. Importantly, introduction of ZEBRA and RTA (to enhance lytic responsiveness) into these cells triggers and recapitulates the EBV lytic cascade (27, 28). We found that, as in EBV$^+$ BL cells, the encapsidated extracellular EBV load following lytic activation was significantly impaired in wild-type Tsg101-expressing p2089 cells exposed to any of the prazoles. However, virus production was rescued in cells expressing the C73A Tsg101 mutant that is refractory to prazole-mediated inhibition (Fig. 6A to C). As expected, expression of siRNA targeting *Tsg101* depleted the pool of endogenous Tsg101 protein but not the siRNA-resistant FLAG-tagged wild-type or C73A mutant Tsg101 (Fig. 6D and E). We conclude that prazoles block EBV capsid egress from the nucleus by interfering directly with Ub binding of the ESCRT-I factor Tsg101 through their interaction with Cys73. Based on previous studies, the mechanism underlying this Tsg101 involvement appears to be unlinked to its well-established role in recruitment of ESCRT-III. If so, further investigation should provide opportunities to gain novel insights into both the EBV egress process and hitherto-unappreciated functions of the Tsg101 protein.

EBV egress from the nucleus is aided by the nuclear egress complex, which is composed of the EBV *BFRF1* and *BFLF2* gene products (29). Indeed, ubiquitination of BFRF1 through the activities of the E3 ligase Itch and the ESCRT-I factor Alix is a required step

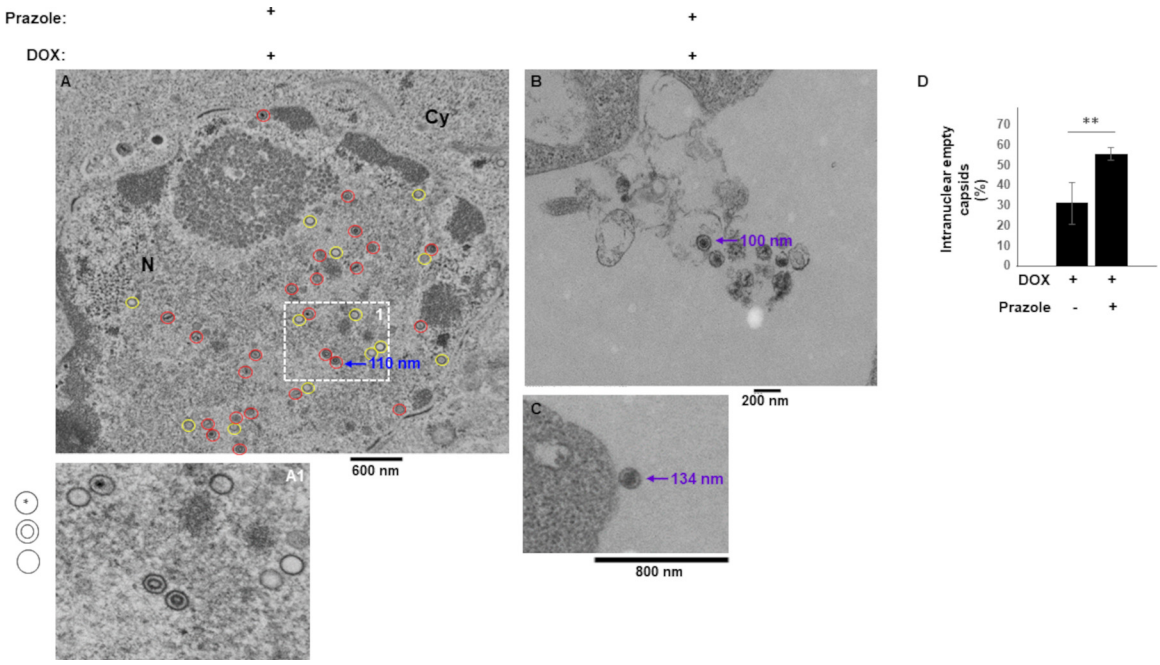

FIG 5 Prazoles negatively impact capsid maturation and size of extracellular virions. CLIX-FZ BL cells were exposed to doxycycline (Dox) plus prazoles. Cells were harvested 48 h later for evaluation by electron microscopy. (A) Numerous nuclear VLPs. Cartoons next to panel A1 indicate the three morphologies shown in panels A and A1. Normal-appearing and defective VLPs are circled in red and yellow, respectively, in panel A. (B and C) Extracellular virions. Sizes of nuclear capsids and extracellular VLPs are also indicated. (D) Percent empty nuclear capsids in doxycycline versus doxycycline plus prazole-treated cells. **, $P < 0.01$.

in BFRF1-mediated modulation of the inner nuclear membrane (11). Notably also, Tsg101 was reported to interact with BFRF1 at the nuclear rim in cells coexpressing BFLF2 (10, 11). The role of Tsg101 was speculated to be indirect (10). Our results provide evidence that Tsg101 plays a direct role in EBV capsid maturation as well as egress from the nucleus. While herpes simplex virus 1 (HSV-1) and human cytomegalovirus, which are alpha- and betaherpesviruses, respectively, exploit the ESCRT-III machinery for nuclear budding, neither seems to require Tsg101 (30, 31). Interestingly, Leis et al. (32) examined prazole efficacy against HSV-1 and HSV-2 and observed a range of susceptibility, with ilaprazole being significantly more effective than tenatoprazole and rabeprazole not being inhibitory at all. As shown here, all three compounds inhibited EBV replication and were effective at concentrations comparable to that found for HSV-1/2 with ilaprazole. Moreover, while ilaprazole and tenatoprazole blocked nuclear egress of HSV-1/2, it appears that the drugs interfere with EBV primary capsid maturation, budding from the nuclear membrane, and transport through the cytoplasmic membranes for ultimate cell egress, events that require ESCRT-III, for which Tsg101 is the conduit. Thus, while HSV-1/2 prazole susceptibility suggests a requirement for the Tsg101-Ub binding event that the drugs inhibit, the observed differences in HSV-1/2 and EBV susceptibility may reflect the extent to which Tsg101 participates directly versus indirectly in the virus assembly process. It should be noted that Kaposi's sarcoma-associated herpesvirus (KSHV), the other human gammaherpesvirus which also causes cancer, uses Tsg101 for entry into the nucleus of endothelial cells (33). Thus, both cancer-causing human herpesviruses may be susceptible to drugs that target Tsg101.

Our results identify three prazoles that are in late-stage clinical trials or already in clinical use for GERD as candidates for alternative use as inhibitors of EBV virion production following lytic reactivation. In contrast to its use as a therapeutic for GERD, where the gastric proton pump that is accessible to the drug at the cell surface is the target, the antiviral activity of prazoles requires prodrug activation inside the cell (8). Virus production dictates infection of new B cells and their unchecked proliferation into life-threatening PTLD under T-cell-immunosuppressive conditions. Similarly,

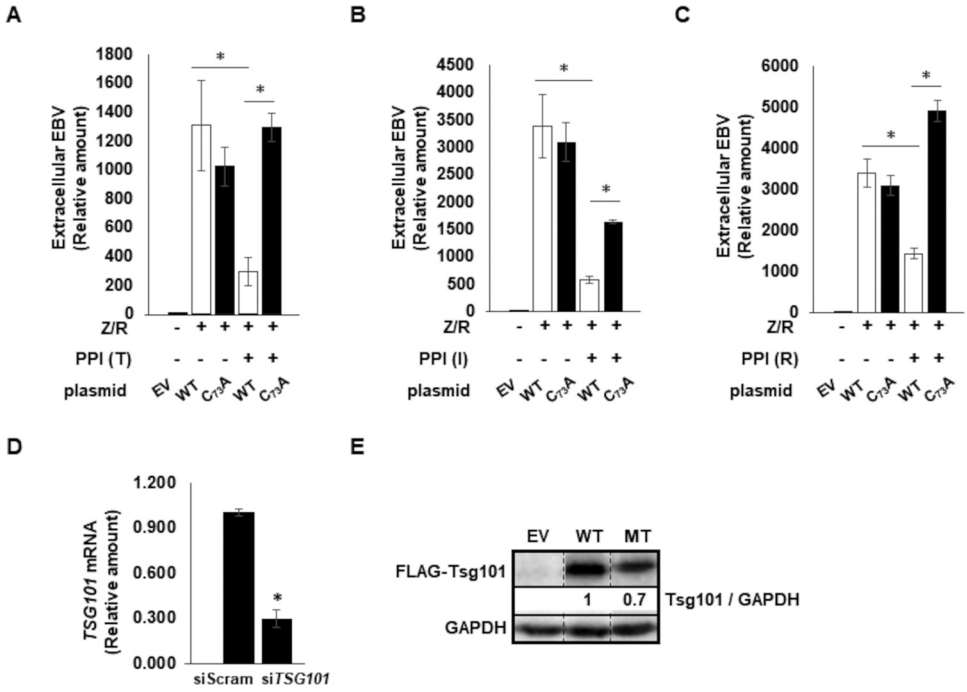

FIG 6 Prazoles inhibit Tsg101-facilitated viral egress. 293T-p2089 cells were exposed to Tsg101 siRNA and empty vector (EV), wild-type (WT) or mutant (MT; C73A) Tsg101 plasmid, plasmids encoding BZLF1 (Z) and BRLF1 (R) to activate the EBV lytic phase, and the prazole tenatoprazole (T), ilaprazole (I), or rabeprazole (R), as indicated. DNase-treated culture supernatants were assayed at 72 h for EBV load using qPCR in panels A to C. Knockdown of *Tsg101* message was assayed by RT-qPCR (D), and expression of FLAG-tagged exogenous Tsg101 was assayed by immunoblotting using anti-FLAG antibody (E). *, $P < 0.05$. Error bars show SEM for technical triplicates from a representative of two independent experiments.

chronic active EBV infection, a debilitating premalignant condition, also relies on the EBV lytic phase. Both disorders could potentially benefit from prazole-mediated suppression of EBV loads, particularly as a prophylactic against PTLD in the early posttransplant period, when the risk of PTLD is the highest. FDA-approved prazoles are widely used to treat acid reflux. Also, importantly, they are orally available and, given their well-established safety and low-toxicity profiles, hold the promise of accelerated repurposing as antiviral agents.

MATERIALS AND METHODS

Cell lines. Cells of the EBV$^+$ Burkitt lymphoma cell line CLIX-FZ (18, 19) bearing a stably integrated doxycycline-inducible *BZLF1* open reading frame (ORF) were cultured in RPMI 1640 (Gibco) supplemented with 10% fetal bovine serum (Alphabioregen) and 1% penicillin-streptomycin (Gibco). A549 cells and HEK293T-p2089 cells (human embryonic kidney cells bearing a wild-type EBV p2089 bacmid) were cultured in F-12 medium (Gibco) and Dulbecco's modified Eagle medium (DMEM) (Gibco), respectively, supplemented with 10% fetal bovine serum and 1% penicillin-streptomycin.

Compounds. Prazole compounds were purchased from Sigma, Toronto Research Chemicals, and Selleck Chemicals. Stock solutions were prepared in dimethyl sulfoxide (DMSO) (100%) and stored in aliquots at −80°C for no longer than 2 months. Prazoles were used at the following concentrations: 40 μM tenatoprazole (T), 10 μM ilaprazole (I), and 10 μM rabeprazole (R).

Induction of EBV lytic cycle. Twenty-four hours after subculture at 4×10^5 ml^{-1}, typically when in logarithmic phase, CLIX-FZ cells were treated with doxycycline at 5 μg/ml to activate the EBV lytic phase.

Flow cytometry. For detection of cells with surface lytic antigens, doxycycline-treated CLIX-FZ cells were stained as described previously (20). Briefly, 48 h after exposure to doxycycline, cells were harvested and incubated (without fixing or permeabilizing) with reference EBV-seropositive or EBV-seronegative human sera for 1 h at room temperature. After three washes, cells were incubated with fluorochrome-conjugated anti-human IgG for another hour at room temperature and subjected to flow cytometry using an Attune NxT flow cytometer (Thermo Fisher). For intracellular staining of BALF5, EA-D, and gp350, cells were fixed and permeabilized as described previously (34), followed by incubation with target-specific antibodies. Antibodies included rabbit anti-BALF5 antibody (MBS1494083; MyBioSource), mouse anti-EA-D antibody (MAB8186; EMD), and mouse anti-gp350 antibody (72A1; ATCC). Data were analyzed using FlowJo software (TreeStar). Analysis gates for flow cytometry were

determined based on parallel staining with reference EBV-seronegative human sera or isotype control antibodies. Pairwise comparisons were made between cells stained with EBV-seropositive and -seronegative sera incubated with various prazoles.

Quantification of EBV in cell culture supernatant. For quantifying released virus, cells were harvested 72 h after treatment with DMSO, doxycycline plus DMSO, or doxycycline plus prazoles (T, I, and R) and separated into cell pellets and supernatant. Supernatants were filtered through a 0.45-μm filter, concentrated and treated with DNase as described previously (19), and evaluated by qPCR using primers targeting EBV BamW, also described previously (35).

RT-qPCR. Reverse transcriptase real-time quantitative PCR (RT-qPCR) was performed using protocols and primers described previously (35). Briefly, total RNA was isolated using an RNeasy kit (Qiagen) followed by DNase digestion (Promega). RNA was quantitated using a NanoDrop instrument (Thermo Scientific). RNA (1 μg) was converted to cDNA by using murine leukemia virus (MuLV) reverse transcriptase (New England Biolabs). Relative transcript levels of selected viral genes were determined with gene-specific primers by using Fast SYBR green master mix on a Quant Studio 3 thermocycler (Applied Biosystems) and analyzed using the $\Delta\Delta C_T$ method. PCR primers included the following: *BZLF1* forward primer, TTCCACAGCCTGCACCAGTG; reverse primer, GGCAGAAGCCACCTCACGGT; *BMRF1* forward primer, ACCTGCCGTTGGATCTTAGTG; reverse primer, GGCGTTGTTGGAGTCCTGTG; and *BLLF1* forward primer, CATGCCGACAAACACCACAG; reverse primer, TTGCGTCCTCAGAAGTGACC.

Cell viability assay. To check cell viability, a water-soluble tetrazolium salt (WST-1) assay was performed as described previously (19). Briefly, CLIX-FZ cells were treated with DMSO, doxycycline, or doxycycline plus prazoles (T, I and R) at 3.3×10^5 ml^{-1} (total, 1 million cells). Twenty-four hours later, cells were seeded in a 96-well plate at 100 μl/well, 10 μl of WST-1 substrate (Sigma no. 5015944001) was added per well, the mixture was incubated at 37°C for 2 h, and absorbance at 450 nm was measured and quantified from each well. In a similar experiment, A549 cells were treated with DMSO and prazoles (T, I, and R) in a 96-well plate; 24 h later, culture medium was changed with 300 μl of fresh F-12/K medium mixed with 33 μl of WST-1 substrate. Two hours later, absorbance at 450 nm was measured.

Electron microscopy. For electron microscopy (EM), 3 million drug-treated CLIX-FZ cells were resuspended in 8.5 ml RPMI in a 15 ml polypropylene tube followed by addition of 8 ml fixative solution. Fixative was prepared by mixing 2 ml EM-grade 16% paraformaldehyde aqueous solution (Fisher Scientific supplier 15710; catalog no. AA433689M), 0.64 ml EM-grade 25% glutaraldehyde aqueous solution (Fisher Scientific supplier 16220, catalog no. 100504-788), and 5.36 ml of PHEM buffer (Fisher Scientific supplier 11162; catalog no. 50-193-1294). Cells in fixative were mixed by inverting the tube a few times before transfer to the EM facility at room temperature. After several buffer washes, cells were postfixed in 1% osmium tetroxide in cacodylate buffer, stained *en bloc* with 1% uranyl acetate, and dehydrated in graded ethanol solutions. Samples were then embedded in EMbed 812 resin (Electron Microscopy Sciences, Hatfield, PA). Ultrathin resin sections were cut and stained with uranyl acetate and lead citrate. Electron microscopy was performed on a JEM 1200 electron microscope (JEOL USA, Peabody, MA) with a bottom-mounted AMT XR-111 digital camera (Advanced Microscopy Techniques Corporation, Woburn, MA).

siRNAs, plasmids, and transfection. To test the involvement of Tsg101 in egress of EBV, siRNA targeting *Tsg101* and FLAG-tagged wild-type or mutant Tsg101 (36) were introduced into HEK293T-p2089 cells induced into the lytic phase by cotransfection of *BZLF1* and *BRLF1* plasmids. siRNA (targeting) directed against *Tsg101* nucleotides 410 to 434 (5′ AGGACGAGAGAAGACTGGAGGTTCA) and control scrambled siRNA were synthesized by Dharmacon. Upon reaching 80% confluence, cells were reseeded in a 6-well plate at 0.3×10^5/well in 2 ml medium. In 2 to 3 days, when cells reached 50% confluence, they were transfected via Lipojet (SignaGen laboratories). Seventy-two hours later, cells were harvested for processing via RT-qPCR and immunoblotting, and supernatants were harvested for measuring viral load by qPCR.

Immunoblotting. Cells were lysed for immunoblotting using radioimmunoprecipitation assay (RIPA) buffer (50 mM Tris-HCl [pH 7.4], 150 mM NaCl, 1% [vol/vol] NP-40, 1% [wt/vol] deoxycholate, 1 mM EDTA, 1× protease, and phosphatase inhibitor cocktail [catalog no. 5872; Cell Signaling Technology]). Cell extracts were electrophoresed in 10% SDS-polyacrylamide gels and transferred onto nitrocellulose membranes. Immunoblotting was performed using antibodies indicated in legend at company-recommended concentrations and conditions.

Statistical analyses. An unpaired *t* test was used to compare the means of two groups of interest.

ACKNOWLEDGMENTS

We thank Xiaofan Li for providing technical guidance.

S.S.M. was supported by the Children's Miracle Network, N.T. was supported by Intramural Research Programs of the National Heart, Lung, and Blood Institute (NHLBI) of the NIH, C.C. was supported by NIH grants R01AI150489 and R21AI139036, and S.B.-M. was supported by NIH grant R01 AI113134, the Children's Miracle Network, and the University of Florida.

S.S.M., C.C., and S.B.-M. designed the study, S.S.M., H.X., and C.K.E.B. acquired the data, S.S.M., N.T., C.C., and S.B.-M. analyzed and interpreted the data, and S.S.M., C.C., and S.B.-M. wrote the manuscript.

We declare that no competing interests exist.

REFERENCES

1. Young LS, Rickinson AB. 2004. Epstein-Barr virus: 40 years on. Nat Rev Cancer 4:757–768. https://doi.org/10.1038/nrc1452.
2. Ahmed I, Akram Z, Iqbal HMN, Munn AL. 2019. The regulation of endosomal sorting complex required for transport and accessory proteins in multivesicular body sorting and enveloped viral budding—an overview. Int J Biol Macromol 127:1–11. https://doi.org/10.1016/j.ijbiomac.2019.01.015.
3. Votteler J, Sundquist WI. 2013. Virus budding and the ESCRT pathway. Cell Host Microbe 14:232–241. https://doi.org/10.1016/j.chom.2013.08.012.
4. Carter CA. 2018. Tumor suppressor gene 101: a virus' multifunctional conduit to the ESCRT trafficking machinery, p 317–351. *In* Parent LJ (ed), Retrovirus-cell interactions. Academic Press, Cambridge, MA.
5. Garrus JE, von Schwedler UK, Pornillos OW, Morham SG, Zavitz KH, Wang HE, Wettstein DA, Stray KM, Cote M, Rich RL, Myszka DG, Sundquist WI. 2001. Tsg101 and the vacuolar protein sorting pathway are essential for HIV-1 budding. Cell 107:55–65. https://doi.org/10.1016/s0092-8674(01)00506-2.
6. Martin-Serrano J, Zang T, Bieniasz PD. 2001. HIV-1 and Ebola virus encode small peptide motifs that recruit Tsg101 to sites of particle assembly to facilitate egress. Nat Med 7:1313–1319. https://doi.org/10.1038/nm1201-1313.
7. VerPlank L, Bouamr F, LaGrassa TJ, Agresta B, Kikonyogo A, Leis J, Carter CA. 2001. Tsg101, a homologue of ubiquitin-conjugating (E2) enzymes, binds the L domain in HIV type 1 Pr55(Gag). Proc Natl Acad Sci U S A 98:7724–7729. https://doi.org/10.1073/pnas.131059198.
8. Watanabe SM, Ehrlich LS, Strickland M, Li X, Soloveva V, Goff AJ, Stauft CB, Bhaduri-McIntosh S, Tjandra N, Carter C. 2020. Selective targeting of virus replication by proton pump inhibitors. Sci Rep 10:4003. https://doi.org/10.1038/s41598-020-60544-y.
9. Sandhu DS, Fass R. 2018. Current trends in the management of gastroesophageal reflux disease. Gut Liver 12:7–16. https://doi.org/10.5009/gnl16615.
10. Lee CP, Liu PT, Kung HN, Su MT, Chua HH, Chang YH, Chang CW, Tsai CH, Liu FT, Chen MR. 2012. The ESCRT machinery is recruited by the viral BFRF1 protein to the nucleus-associated membrane for the maturation of Epstein-Barr Virus. PLoS Pathog 8:e1002904. https://doi.org/10.1371/journal.ppat.1002904.
11. Lee CP, Liu GT, Kung HN, Liu PT, Liao YT, Chow LP, Chang LS, Chang YH, Chang CW, Shu WC, Angers A, Farina A, Lin SF, Tsai CH, Bouamr F, Chen MR. 2016. The ubiquitin ligase Itch and ubiquitination regulate BFRF1-mediated nuclear envelope modification for Epstein-Barr virus maturation. J Virol 90:8994–9007. https://doi.org/10.1128/JVI.01235-16.
12. Koonin EV, Abagyan RA. 1997. TSG101 may be the prototype of a class of dominant negative ubiquitin regulators. Nat Genet 16:330–331. https://doi.org/10.1038/ng0897-330.
13. Ponting CP, Cai YD, Bork P. 1997. The breast cancer gene product TSG101: a regulator of ubiquitination? J Mol Med (Berl) 75:467–469.
14. Henne WM, Buchkovich NJ, Emr SD. 2011. The ESCRT pathway. Dev Cell 21:77–91. https://doi.org/10.1016/j.devcel.2011.05.015.
15. Strickland M, Ehrlich LS, Watanabe S, Khan M, Strub MP, Luan CH, Powell MD, Leis J, Tjandra N, Carter CA. 2017. Tsg101 chaperone function revealed by HIV-1 assembly inhibitors. Nat Commun 8:1391. https://doi.org/10.1038/s41467-017-01426-2.
16. Goff A, Ehrlich LS, Cohen SN, Carter CA. 2003. Tsg101 control of human immunodeficiency virus type 1 Gag trafficking and release. J Virol 77:9173–9182. https://doi.org/10.1128/jvi.77.17.9173-9182.2003.
17. Watanabe SM, Strickland M, Tjandra N, Carter CA. 2020. RNA binding suppresses Tsg101 recognition of Ub-modified Gag and facilitates recruitment to the plasma membrane. Viruses 12:447. https://doi.org/10.3390/v12040447.
18. Li X, Burton EM, Bhaduri-McIntosh S. 2017. Chloroquine triggers Epstein-Barr virus replication through phosphorylation of KAP1/TRIM28 in Burkitt lymphoma cells. PLoS Pathog 13:e1006249. https://doi.org/10.1371/journal.ppat.1006249.
19. Li X, Akinyemi IA, You JK, Rezaei MA, Li C, McIntosh MT, Del Poeta M, Bhaduri-McIntosh S. 2020. A mechanism-based targeted screen to identify Epstein-Barr virus-directed antiviral agents. J Virol 94:e01179-20. https://doi.org/10.1128/JVI.01179-20.
20. Bhaduri-McIntosh S, Miller G. 2006. Cells lytically infected with Epstein-Barr virus are detected and separable by immunoglobulins from EBV-seropositive individuals. J Virol Methods 137:103–114. https://doi.org/10.1016/j.jviromet.2006.06.006.
21. Daigle D, Megyola C, El-Guindy A, Gradoville L, Tuck D, Miller G, Bhaduri-McIntosh S. 2010. Upregulation of STAT3 marks Burkitt lymphoma cells refractory to Epstein-Barr virus lytic cycle induction by HDAC inhibitors. J Virol 84:993–1004. https://doi.org/10.1128/JVI.01745-09.
22. Shin JM, Homerin M, Domagala F, Ficheux H, Sachs G. 2006. Characterization of the inhibitory activity of tenatoprazole on the gastric H+,K+-ATPase in vitro and in vivo. Biochem Pharmacol 71:837–849. https://doi.org/10.1016/j.bcp.2005.11.030.
23. Christ L, Raiborg C, Wenzel EM, Campsteijn C, Stenmark H. 2017. Cellular functions and molecular mechanisms of the ESCRT membrane-scission machinery. Trends Biochem Sci 42:42–56. https://doi.org/10.1016/j.tibs.2016.08.016.
24. Vietri M, Radulovic M, Stenmark H. 2020. The many functions of ESCRTs. Nat Rev Mol Cell Biol 21:25–42. https://doi.org/10.1038/s41580-019-0177-4.
25. Nanbo A, Noda T, Ohba Y. 2018. Epstein-Barr virus acquires its final envelope on intracellular compartments with Golgi markers. Front Microbiol 9:454. https://doi.org/10.3389/fmicb.2018.00454.
26. Leis J, Luan CH, Audia JE, Dunne SF, Heath CM. 2020. Ilaprazole and other novel prazole-based compounds that bind Tsg101 inhibit viral budding of HSV-1/2 and HIV from cells. bioRxiv https://doi.org/https://doi.org/10.1101/2020.05.04.075036.
27. Yu X, Wang Z, Mertz JE. 2007. ZEB1 regulates the latent-lytic switch in infection by Epstein-Barr virus. PLoS Pathog 3:e194. https://doi.org/10.1371/journal.ppat.0030194.
28. Feederle R, Kost M, Baumann M, Janz A, Drouet E, Hammerschmidt W, Delecluse HJ. 2000. The Epstein-Barr virus lytic program is controlled by the co-operative functions of two transactivators. EMBO J 19:3080–3089. https://doi.org/10.1093/emboj/19.12.3080.
29. Lake CM, Hutt-Fletcher LM. 2004. The Epstein-Barr virus BFRF1 and BFLF2 proteins interact and coexpression alters their cellular localization. Virology 320:99–106. https://doi.org/10.1016/j.virol.2003.11.018.
30. Pawliczek T, Crump CM. 2009. Herpes simplex virus type 1 production requires a functional ESCRT-III complex but is independent of TSG101 and ALIX expression. J Virol 83:11254–11264. https://doi.org/10.1128/JVI.00574-09.
31. Tandon R, AuCoin DP, Mocarski ES. 2009. Human cytomegalovirus exploits ESCRT machinery in the process of virion maturation. J Virol 83:10797–10807. https://doi.org/10.1128/JVI.01093-09.
32. Leis J, Luan CH, Audia JE, Dunne SF, Heath CM. 2021. Ilaprazole and other novel prazole-based compounds that bind Tsg101 inhibit viral budding of HSV-1/2 and HIV from cells. J Virol https://doi.org/10.1128/JVI.00190-21. Epub ahead of print.
33. Kumar B, Dutta D, Iqbal J, Ansari MA, Roy A, Chikoti L, Pisano G, Veettil MV, Chandran B. 2016. ESCRT-I protein Tsg101 plays a role in the post-macropinocytic trafficking and infection of endothelial cells by Kaposi's sarcoma-associated herpesvirus. PLoS Pathog 12:e1005960. https://doi.org/10.1371/journal.ppat.1005960.
34. Hill ER, Koganti S, Zhi J, Megyola C, Freeman AF, Palendira U, Tangye SG, Farrell PJ, Bhaduri-McIntosh S. 2013. Signal transducer and activator of transcription 3 limits Epstein-Barr virus lytic activation in B lymphocytes. J Virol 87:11438–11446. https://doi.org/10.1128/JVI.01762-13.
35. Burton EM, Goldbach-Mansky R, Bhaduri-McIntosh S. 2020. A promiscuous inflammasome sparks replication of a common tumor virus. Proc Natl Acad Sci U S A 117:1722–1730. https://doi.org/10.1073/pnas.1919133117.
36. Lu Q, Hope LW, Brasch M, Reinhard C, Cohen SN. 2003. TSG101 interaction with HRS mediates endosomal trafficking and receptor down-regulation. Proc Natl Acad Sci U S A 100:7626–7631. https://doi.org/10.1073/pnas.0932599100.